Spatial-Temporal Resource Optimization for Uneven-Traffic LEO Satellite Systems: Beam Pattern Selection and User Scheduling

Lei Lei, *Member, IEEE,* Anyue Wang, Eva Lagunas, *Senior Member, IEEE,* Xin Hu, *Senior Member, IEEE,* Zhengquan Zhang, *Member, IEEE,* Zhiqiang Wei, *Member, IEEE,* Symeon Chatzinotas, *Fellow, IEEE*

***Abstract*—With the commercial deployment of low earth orbit (LEO) satellites, the future integrated 6G-satellite system represents an excellent solution for ubiquitous connectivity and high-throughput data service to massive users. Due to the heterogeneity of users' traffic profiles, uneven traffic distribution among beams or users often occurs in LEO satellite systems. Conventional satellite payloads with fixed beam radiation patterns may result in large gaps between requested and allocated capacity. The advances of flexible satellite payloads with dynamic beamforming capabilities enable spot beams to adjust their coverage and adaptively schedule users, thus offering spatial-temporal domain flexibility. Motivated by this, as an early attempt, we investigate how adaptive beam patterns with flexible user scheduling schemes can help alleviate mismatches of requested-transmitted data in uneven-traffic and full-frequency reuse LEO systems. We formulate an optimization problem to jointly determine beam patterns, power allocation, user-LEO association, and user-slot scheduling. The problem is identified as mixed-integer nonconvex programming. We propose an efficient iterative algorithm to solve the problem by first determining beam patterns and user associations at the frame scale, followed by optimizing power allocation and user scheduling at the timeslot scale. The four-decision components are iteratively updated to improve the overall performance. Numerical results demonstrate the benefits brought by adaptive beam patterns and their effectiveness in reducing the mismatch effect in uneven-traffic LEO systems.**

***Index Terms*—Low earth orbit (LEO) satellite, uneven traffic, adaptive beam radiation patterns, resource optimization.**

This work was supported in part by the Open Research Fund of National Mobile Communications Research Laboratory of Southeast University under grant 2023D02; in part by the National Key Laboratory Foundation under grant 2023-JCJQ-LB-007; in part by the National Natural Science Foundation of China (NSFC) project under Grant 61871334 and Grant U2268201; in part by the Luxembourg National Research Fund (FNR) MegaLEO project under grant C20/IS/14767486; in part by the Natural Science Foundation of Sichuan Province under grant 2023NSFSC0455; in part by the major key project of Peng Cheng Laboratory under grant PCL2023AS1-2. (Corresponding author: Zhiqiang Wei)

L. Lei is with the School of Information and Communications Engineering, Xi'an Jiaotong University, 710049 Xi'an, China, and also with the National Mobile Communications Research Laboratory, Southeast University, Nanjing 210096, China (email: lei.lei@xjtu.edu.cn).

A. Wang, E. Lagunas, and S. Chatzinotas are with Interdisciplinary Center for Security, Reliability and Trust, University of Luxembourg, 1855 Luxembourg (email: anyue.wang; eva.lagunas; symeon.chatzinotas@uni.lu).

X. Hu is with the School of Electronic Engineering, Beijing University of Posts and Telecommunications, Beijing 100876, China (email: huxin2016@bupt.edu.cn).

Z. Zhang is with Southwest Jiaotong University, Chengdu, China.

Z. Wei is with the School of Mathematics and Statistics, Xi'an Jiaotong University, Xi'an 710049, China, and also with the Peng Cheng Laboratory, Shenzhen, Guangdong 518055, China, and also with the Pazhou Laboratory (Huangpu), Guangzhou, Guangdong 510555, China (e-mail: zhiqiang.wei@xjtu.edu.cn).

Part of this paper has been presented at IEEE Globecom, Dec. 2022. [20]

I. Introduction

LOW earth orbit (LEO) satellite systems are envisioned as one of the promising solutions to the upcoming beyond 5G (B5G) and 6G era for the potentials of offering high-throughput transmission and extending communications to remote or unserved areas [1]. Compared to geostationary earth orbit (GEO) and and medium earth orbit (MEO) satellites, LEO satellites operate at lower altitudes with low latency and transmission attenuation [2]. To address exponentially growing traffic demand and support ubiquitous connectivity in the future, the industry is motivated to develop projects on building advanced architectures with hundreds or thousands of LEO satellites in space [3].

The dense deployment of LEO satellites may introduce more interference. users, especially those located in the areas overlapped by neighboring satellites' beam coverages, may receive considerable co-channel interference, which could result in severe performance degradation [4], [5]. Another typical concern is raised by the heterogeneity of traffic distribution that often varies temporally and geographically. To improve the utilization of scarce spectrum, resource allocation in LEO satellite systems shall be adapted to the dynamic variations of on-ground traffic demand [6]. The coordination of multiple LEO satellites to provide high-quality services to ground users is crucial and challenging, which calls for the introduction of more flexibility in radio resource allocation.

In conventional satellite systems, beam radiation patterns are decided before launch and the projected beam shapes (or footprints) are fixed during service [7]. As the deployment of LEO satellites becomes dense, the fixed footprint plan cannot adapt to dynamic variations and uneven traffic distribution, which limits the performance. With the advances of flexible payloads with onboard digital processing, beam shapes can be dynamically altered by changing beam patterns via beamforming networks (BFN) instead of mechanically moving antennas [7]–[9]. By adjusting the selection of different beam patterns, data transmission in satellite systems can be more adaptive to non-uniform traffic distribution and with mitigated co-channel interference [10], [12], [14]. Besides, the capability of integrating to terrestrial systems or non-terrestrial networks (NTN) can be improved by adapting footprints to reduce co-channel interference to terrestrial systems [16] or to satisfy configuration requirements in various systems [17]. The authors in [18] developed a multi-objective deep reinforcement

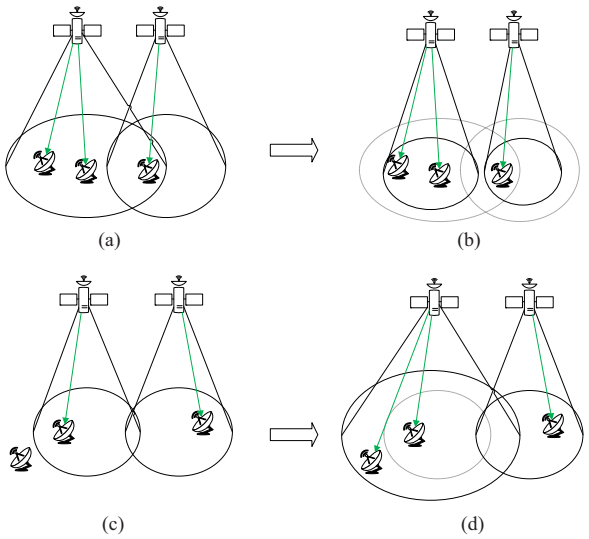

Fig. 1: Illustrative examples of adjusting beam patterns for better coverage and efficient transmission. Reducing coverage areas from (a) to (b) to avoid overlap and mitigate co-channel interference; Enlarging coverage areas from (c) to (d) to connect more users.

learning approach for dynamic beam hopping to reduce the gap of offered-allocated capacity. Illustrative instances of adaptive beam patterns are shown in Fig. 1. When a user is located in the area covered by two adjacent satellite beams (full frequency reuse), e.g., in Fig. 1(a), it may suffer from large inter-satellite interference. To reduce the interference, both satellites could select beam patterns with smaller coverage to avoid overlap, as depicted in Fig. 1(b). Another typical example is to change patterns with wider radiated beams to cover more users that are beyond but near the beam edge, as presented in the process from Fig. 1(c) to Fig. 1(d).

A. Related Works

Considering extra flexibility in spatial domain and advantages of traffic adaptation and interference mitigation, the design of adaptive beam pattern schemes has received growing attention. In [16], the authors studied adaptive beam control schemes in LEO satellite systems to maximize the signal-to-noise ratio and minimize the interference to incumbent terrestrial systems. The authors in [10] jointly optimized beam size and transmit power to improve the adaptation to varying traffic. Particularly, the coupling between beamwidth and power was discussed. In [11], the authors designed flexible schemes to tackle several issues for satellite systems, including beam localization, beamwidth adjustment, use-beam scheduling, and beam coloring. Besides beam size, more factors affecting beam shapes, e.g., beam center and rotation angle, were taken into account, and novel footprint planning strategies were designed to match offered capacity to irregular traffic distribution in [12]. Further, the authors in [13] provide a more comprehensive view on beam radiation pattern design, considering factors like beamwidth, beam center, required effective isotropic radiated power, side lobe levels, and nulling direction. In the above works, regular beam shapes (e.g., circular or elliptical) were employed. However, the expressions of transmit antenna gain w.r.t. configuration parameters (including beamwidth, beam center, rotation angle, etc.) are generally sophisticated [12]. Directly defining the optimal beam pattern is difficult and cumbersome, even when we consider regular beam shapes. These approaches may also be inapplicable to more general scenarios where irregular beam shapes are adopted [7]. Regarding irregular shaped beams, the authors in [15], provided a generic radiation model and designed a dynamic beamforming optimization framework to adjust offered capacity to match irregular traffic demands.

Unlike the above works that directly optimize beam radiation patterns, multiple candidate beam patterns can be pre-designed and the corresponding parameter settings can be stored in advance for various potential scenarios [19]. During service, suitable beam patterns can be selected from the candidate set depending on traffic distribution and interference levels. Unlike directly optimizing beam patterns, the optimization of beam pattern selection can be applied to any type of footprint. Additionally, the update of candidate beam patterns can be processed ahead of transmission rather than real-time adjustment, which is more extendable to practical implementation. In [14], the authors optimized beam pattern selection to minimize the capacity-demand gap, normalized coverage error, and cost per Gbps in orbits and discussed the implementation of adaptive beam patterns in practical satellite payloads.

B. Motivations and Contributions

The abovementioned works focused on optimizing beam patterns from the beam level, i.e., satisfying irregular traffic distribution across different areas rather than capacity-demand matching for specific users. The mutual influence between adaptive beam patterns and resource allocation (e.g., power allocation and user association/scheduling) has not been fully discussed. For instance, when the beam pattern plan is aggressive with large footprints, more users can be covered by the footprint. However, the co-channel interference, especially for users in the overlapped areas, becomes larger, leading to difficulties in resource allocation. On the contrary, the effect of interference is eased to some extent when narrow beams are employed, and thus a more flexible scheduling plan can be applied. Not all the users are covered by their associated beams and thus low data rate may happen to those edge users. In this case, the performance of resource allocation would be limited by inappropriate beam pattern selection.

As an early-attempt study in [20], we evaluate the performance gain of adopting adaptive beam pattern in LEO satellite systems under pre-decided user scheduling. For extension, we are motivated to provide more comprehensive insights on joint resource optimization of beam pattern selection and resource allocation and aim to analyze their mutual influence, which distinguish this work from other state-of-the-art works [10], [12], [14], [15]. The main contributions are summarized as follows:

- To investigate the coupling between beam pattern selection and resource allocation in LEO satellite systems, we formulate a joint optimization problem of beam pattern

selection, power allocation, user-LEO association, and user-slot scheduling. The objective is to minimize the capacity-demand gap such that the delivered data can be matched to users' uneven traffic demands.

- We provide insights on determining beam patterns and user association via thoroughly analyzing a special case. That is, satellites tend to serve high-demand users and select narrow beams, more concentrated on associated users and radiating less interference to other users.
- We propose an efficient scheme to jointly optimize power allocation and user scheduling on a timeslot-by-timeslot basis.
- We design a swap-based approach to update pattern selection and user association such that the performance can be iteratively improved.
- Numerical results demonstrate the advantages of adaptive beam patterns over conventional single-pattern schemes. The results validate the performance of the proposed scheme in terms of complexity, capacity-demand matching, power consumption, and user association over benchmarks.

The remainders of the paper are organized as follows: Section II elaborates the considered LEO satellite systems with the functionality of adaptive beam patterns. In Section III, we formulate a joint optimization problem of power allocation, beam pattern selection, and user association/scheduling. In Section IV, we analyze the optimization of beam pattern selection and user association. An efficient approach of jointly optimizing power allocation and user scheduling is provided in Section V. In this section, we also present a swap-based approach to further improve the performance. Numerical results are presented and analyzed in Section VI. Section VII concludes the paper.

II. System Model

Consider downlink data transmission in a LEO satellite system, as depicted in Fig. 2. S LEO satellites fly over the area of interest, where each satellite beam's coverage may be partially overlapping with neighboring beams. Denote $\mathcal{S}$ as the set of the satellites and $\mathcal{K}$ as the set of the users. We assume that each LEO satellite generates one beam [5], [16], [17]. In the system, all the LEO satellites fully reuse the same frequency band. The communication procedure is described as follows: First, messages containing users' status, e.g., channel conditions, traffic demand, users' positions, etc., are fed back to the gateway via return links. Based on the information, the resource manager co-located with the gateway executes the resource optimization algorithm to generate optimized decisions, including beam pattern selection, user association/scheduling, and power allocation. Note that beam configurations can be communicated through the TT&C link in practice which can be separate from the feeder link. Next, the gateway informs the decisions to satellites and delivers data from the core networks to satellites. At last, satellites generate beams according to the selected patterns and transmit data to targeted users. Remark that the latency among different transmission links is assumed to be identical.

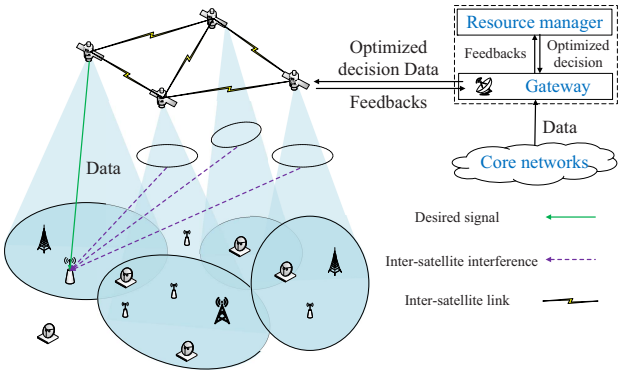

Fig. 2: An illustrative scenario of the considered LEO satellite system where adaptive beam patterns are adopted.

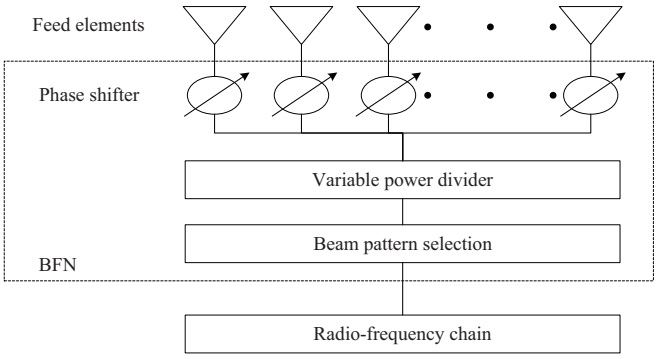

Fig. 3: The shaped beam antenna with BFN.

Denote $\mathcal{N}_s$ as the set of the candidate beam patterns of satellite s. Each pattern corresponds to one specific beam shape. With optimized decisions informed by the gateway, one beam pattern is selected from $\mathcal{N}_s$. The information of resource allocation is carried before the data frame is transmitted. In practical satellite systems, the communication distances between satellites and ground terminals are large and the latency may not be ignored. We consider that beam patterns and user association change on a frame-by-frame basis and resource allocation is targeted for one frame. Denote $\mathcal{T}$ as the set of the T timeslots in one frame. The beam pattern is generated by the BFN on the satellite payload, as depicted in Fig. 3. By BFN controlling phase shifters and variable power dividers to alter phases and amplitudes, respectively, each feed element generates one elementary beam and the shaped beam is constructed by these elementary beams [7]. The resulted beam shape is defined as the coverage within the φ-dB contour [7].

The relationship between the transmit antenna gain of a beam pattern and the corresponding configuration parameters is sophisticated and might not be captured by explicit expressions, especially for patterns with irregular beam shapes [7], [12], [14]. For illustration, we plot the 3dB curve to produce ellipse beams to illustrate the beam pattern model. The transmit antenna gain of satellite s with beam pattern n regarding user k is expressed by,

$$G_{snk}^{\mathrm{Tx}} = G_{sn,\max}^{\mathrm{Tx}} \left(\frac{J_1(u_{snk})}{2u_{snk}} + 36 \frac{J_3(u_{snk})}{u_{snk}^3} \right)^2, \qquad (1)$$

where $J_1(\cdot)$ and $J_3(\cdot)$ are Bessel functions of the first kind of order one and three, respectively. $G^{\mathrm{Tx}}_{sn,\max}$ is the peak transmit antenna gain of satellite s with pattern n. The notation u_{snk} is expressed as,

$$u_{snk} = 2.07123\frac{\sin\theta_{sk}}{\sin\theta_{sn,3\mathrm{dB}}}, \tag{2}$$

where θ_{sk} denotes the off-axis angle between the s-th satellite's beam center and the k-th user. $\theta_{sn,3\mathrm{dB}}$ denotes the 3-dB angular beamwidth of pattern n radiated by satellite s. The beam pattern model in (1) is widely adopted, e.g., a simplified Bessel function was adopted in 3GPP TR 38.811 [21].

For other types of beam shapes, the expression could be more complicated, e.g., the transmit antenna gain for elliptical beams depends on beam center position, beamwidth (including the major and minor axes), and tilt angle [7], [12]. Remark that we only focus on beam pattern selection, where the candidate patterns are determined before transmission and can be updated easily when necessary. Thus the approaches discussed in this paper can be applied to any types of footprints.

The channel loss from satellite s to user k is written as [21],

$$[L^{\mathrm{total}}_{sk}] = [L^{\mathrm{ba}}_{sk}] + [L^{\mathrm{ga}}_{sk}] + [L^{\mathrm{sc}}_{sk}] + [L^{\mathrm{ra}}_{sk}], \tag{3}$$

where L^{ga}_{sk}, L^{sc}_{sk}, and L^{ra}_{sk} are gaseous, scintillation, and rain attenuation exceeded for $\rho\%$ of an average year, respectively. Here, the operator $[\cdot]$ converts values into dB. L^{ba}_{sk} is the basic path loss, which is derived as,

$$[L^{\mathrm{ba}}_{sk}] = [L_{sk}] + [L^{\mathrm{sf}}_{sk}], \tag{4}$$

where L^{sf}_{sk} denotes shadow fading following log-normal distribution. L_{sk} denotes the free-space path loss, which is expressed by [20],

$$L_{sk} = 32.45 + 20\log_{10}(f^{\mathrm{freq}}) + 20\log_{10}(d_{sk}), \tag{5}$$

where d_{sk} is the distance from satellite s to user k, and f^{freq} is the frequency. The channel gain from satellite s to user k with beam pattern n is expressed as,

$$|h_{skn}|^2 = G^{\mathrm{Tx}}_{skn} G^{\mathrm{Rx}}_{k} / L^{\mathrm{total}}_{sk}, \tag{6}$$

where G^{Rx}_{k} is the receive antenna gain of user k. The channel gain from satellite s to user k is derived as,

$$|h_{sk}|^2 = \sum_{n\in\mathcal{N}_s} y_{sn}|h_{skn}|^2. \tag{7}$$

Here, $y_{sn} \in \{0,1\}$ indicates beam pattern selection, where $y_{sn} = 1$ if satellite s selects the n-th pattern and $y_{sn} = 0$ otherwise.

If user k associated to satellite s is scheduled at timeslot t, the corresponding signal-to-interference-plus-noise ratio (SINR) is expressed as,

$$\gamma_{skt} = \frac{\sum\limits_{n\in\mathcal{N}_s} y_{sn}|h_{skn}|^2 P_{st}}{\sum\limits_{s'\in\mathcal{S}\setminus\{s\}}\sum\limits_{n\in\mathcal{N}_{s'}} y_{s'n}|h_{s'kn}|^2 P_{s't} + \sigma^2}, \tag{8}$$

where P_{st} is the transmit power of satellite s at timeslot t and σ^2 is the noise power. The available rate of user k if scheduled by satellite s at timeslot t is,

$$R_{skt} = B\log(1+\gamma_{skt}), \tag{9}$$

where B is bandwidth. The offered capacity (in bps) of user k is,

$$R_k = \sum_{t\in\mathcal{T}}\sum_{s\in\mathcal{S}} x_{skt} R_{skt}, \tag{10}$$

where $x_{skt} \in \{0,1\}$ indicates whether the user is scheduled to timeslot t by satellite s ($x_{skt} = 1$ if scheduled and 0 otherwise).

III. Problem Formulation

We formulate a resource allocation problem to jointly optimize power allocation, beam-pattern selection, and user association and scheduling. The optimization variables are listed as follows,

$P_{st} \geq 0$, transmit power of satellite s at timeslot t;

$$x_{skt} = \begin{cases} 1, & \text{if satellite } s \text{ serves user } k \text{ at timeslot } t, \\ 0, & \text{otherwise;} \end{cases}$$

$$y_{sn} = \begin{cases} 1, & \text{if satellite } s \text{ selects the } n\text{-th beam pattern,} \\ 0, & \text{otherwise;} \end{cases}$$

$$z_{sk} = \begin{cases} 1, & \text{if user } k \text{ is associated to satellite } s, \\ 0, & \text{otherwise.} \end{cases}$$

The objective is to minimize the sum of capacity-demand gap, which is measured by $\sum_{k\in\mathcal{K}}|R_k - D_k|$. This dissimilarity metric has been widely adopted in satellite systems, which can describe the mismatch effects between offered capacity and requested traffic. Note that the case $R_k = D_k$ reflects a perfect capacity-demand match and the gap increases if R_k is distant from D_k (either larger or smaller). The optimization problem is formulated as,

$$\mathcal{P}_0: \min_{P_{st},x_{skt},y_{sn},z_{sk}} \sum_{k\in\mathcal{K}} |R_k - D_k| \tag{11a}$$

$$\text{s.t. } P_{st} \leq \bar{P}_s, \forall s\in\mathcal{S}, \forall t\in\mathcal{T}, \tag{11b}$$

$$\sum_{s\in\mathcal{S}} z_{sk} \leq 1, \forall k\in\mathcal{K}, \tag{11c}$$

$$\sum_{k\in\mathcal{K}} z_{sk} \leq \widetilde{K}_s, \forall s\in\mathcal{S}, \tag{11d}$$

$$\sum_{k\in\mathcal{K}} x_{skt} = 1, \forall s\in\mathcal{S}, \forall t\in\mathcal{T}, \tag{11e}$$

$$x_{skt} \leq z_{sk}, \forall s\in\mathcal{S}, \forall k\in\mathcal{K}, \forall t\in\mathcal{T}, \tag{11f}$$

$$\sum_{n\in\mathcal{N}_s} y_{sn} = 1, \forall s\in\mathcal{S}, \tag{11g}$$

$$R_k \geq R^{\min}_k \sum_{s\in\mathcal{S}} z_{sk}, \forall k\in\mathcal{K}. \tag{11h}$$

In (11b), the transmit power of satellites is no larger than the power budget. In (11c), each user can be associated to at most one satellite. For the s-th satellite, at most $\widetilde{K}_s$ users can be associated in (11d). In (11e), each satellite schedules only one user to each timeslot. The connection between x_{skt} and z_{sk} is expressed in (11f). If user k is not associated to satellite s, i.e., $z_{sk} = 0$, x_{skt} is restricted to zero; otherwise, $x_{skt} \in \{0,1\}$. Constraints (11g) restrict that each satellite can only select one pattern. In (11h), the offered capacity of user k should

be at least larger than $R_k^{\min}$ if the user is associated to any satellite. Usually, the requested traffic demand is larger than the minimum-rate requirement, i.e., $D_k > R_k^{\min}$.

We can observe that $\mathcal{P}_0$ falls into the category of mixed-integer nonconvex programming considering the non-convexity of the objective function and constraints (11h) (resulted by the non-convex expression of R_{skt} in (8) and (9)) and the presence of binary variables x_{skt}, y_{sn}, and z_{sk}. It is a non-trivial task to directly solve $\mathcal{P}_0$. To tackle the problem, we decompose the original problem into two subproblems: 1) joint optimization of beam pattern selection and user association; 2) joint optimization of power allocation and user scheduling.

IV. Joint Optimization of Beam Pattern Selection and User Association

In this section, we study beam pattern selection and user association. The joint problem of beam pattern selection and user association is expressed as,

$$\mathcal{P}_1: \min_{y_{sn}, z_{sk}} \sum_{k \in \mathcal{K}} |R_k - D_k| \tag{12a}$$

$$\text{s.t. } (11c), (11d), (11f), (11g), (11h). \tag{12b}$$

Since the binary variables y_{sn} appear in both numerator and denominator of the SINR expression as shown in (8), $\mathcal{P}_1$ is non-convex integer programming, which is difficult to solve. We first study the characteristics of $\mathcal{P}_1$ by discussing strategies in some special cases. Based on the analysis, we design an approach to determine beam patterns and user association.

A. Discussion of Special Cases

Consider a scenario in Fig. 4 in which multiple LEO satellites aim to serve an area with heterogeneous traffic distribution. In the first case, satellites move to the positions where high-demand users are located near the beam center, as depicted in Fig. 4(a). Since high-demand users' performance is more significant to the capacity-demand matching of the whole system compared to low-demand users, satellites tend to select beam patterns with smaller but more concentrated shapes, e.g., in Fig. 4(b). In this way, more capacity is offered to high-demand users and meanwhile co-channel interference towards other beams is mitigated, such that the capacity-demand mismatch can be largely reduced.

As satellites move to the right, however, the distances between satellites and users change. High-demand users stand beyond the beam coverage much worse channel conditions, resulting in deteriorated performance even if more resources are assigned to them. In this case, satellites are prone to expand their beam coverage to serve more low-demand users but with better channel conditions to reduce mismatch effects, as shown in Fig. 4(c).

From the above special cases, we observe that the decision of beam pattern selection and user association is influenced by users' demand and channel conditions. Based on the above cases, we discuss how to optimize beam pattern selection and user association in the following remark.

Remark 1: The optimization of beam pattern selection and user association is discussed from the following two aspects:

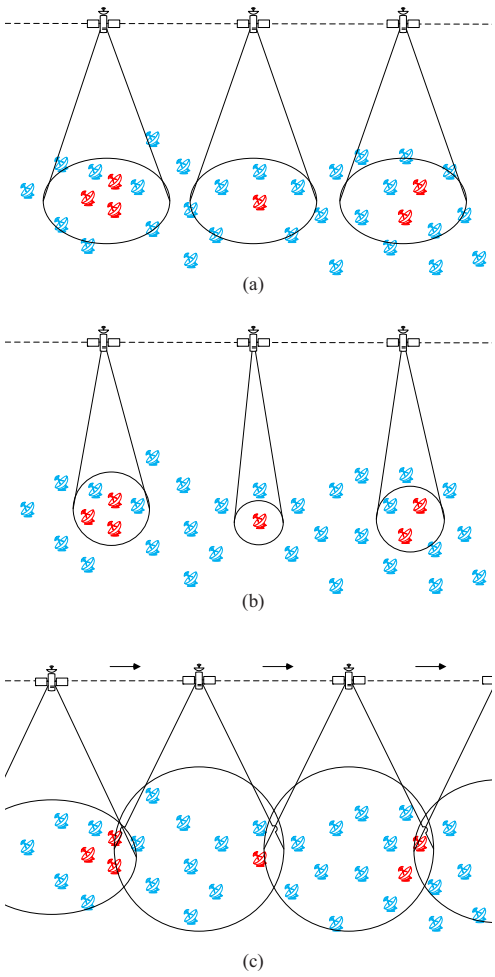

Fig. 4: Illustration of the special-case scenario, where multiple LEO satellites are flying (from the left to the right) over the targeted area with heterogeneous traffic distribution. High-demand and low-demand users are colored in red and blue, respectively. Depending on different traffic distributions within the beam coverage, satellites adjust their selections of beam patterns and associated users.

- *User association: Given determined beam patterns, the decisions of association is made by considering both users' demand and channel conditions. On the one hand, users with higher demand are more likely to be served since they have more influence on the overall capacity-demand gap. On the other hand, satellites tend to choose users experiencing better channel conditions, i.e., larger gain from the associated satellite but smaller inter-satellite interference.*
- *Beam pattern selection: With the decision of user association, each satellite selects a beam pattern generating large channel gains to the associated users but small co-channel interference to users served by neighboring satellites.* □

In short, *Remark 1* conveys that satellites tend to select patterns with smaller but concentrated beams to cover the associated users as well as generate smaller inter-satellite interference and select users for association with higher demand and better channel conditions.

Algorithm 1 Optimization of beam pattern selection and user association

Input: $|h_{skn}|^2$, D_k. Initialized y_{sn}, z_{sk}.

1: **repeat**
2: Calculate μ_{sk} in (13), $\forall k \in \mathcal{K}$, $\forall s \in \mathcal{S}$.
3: Sort μ_{sk} for each satellite.
4: Each satellite selects $\widetilde{K}$ largest-μ_{sk} users for association.
5: Update z_{sk} and $\mathcal{K}_s$.
6: Computes ν_{sn} in (14), $\forall n \in \mathcal{N}_s$, $\forall s \in \mathcal{S}$.
7: Each satellite selects the pattern with the largest ν_{sn}.
8: Update y_{sn}.
9: **until** y_{sn} and z_{sk} converge or reaching I_1 iterations

Output: Optimized y_{sn}, z_{sk}.

B. Algorithmic Design

Based on *Remark 1*, we design an approach to determine user association and beam pattern selection. Given beam pattern selection, we calculate the following ratios,

$$\mu_{sk} = D_k \log\left(\frac{|h_{sk}|^2}{\sum\limits_{s' \in \mathcal{S}\setminus\{s\}} |h_{s'k}|^2}\right), \forall k \in \mathcal{K}, \forall s \in \mathcal{S}, \quad (13)$$

which take into consideration both channel conditions and traffic demands. By sorting these ratios, each satellite selects $\widetilde{K}$ largest-μ_{sk} users for association and update $\mathcal{K}_s$ (the set of users associated to satellite s). After deciding user association, each satellite computes the following ratios,

$$\nu_{sn} = \sum_{k \in \mathcal{K}_s} \frac{|h_{skn}|^2}{\sum\limits_{k \in \mathcal{K}_{s'}, s' \neq s} |h_{sk'n}|^2}, \forall n \in \mathcal{N}_s, \forall s \in \mathcal{S}, \quad (14)$$

for each beam pattern and selects the pattern with the largest ν_{sn}, i.e., largest gain from satellite s but smallest interference to users associated to $s' \neq s$.

The whole procedure is summarized in Alg. 1, where user association is decided in line 2 to line 5 and beam pattern selection is proceeded in line 6 to line 8. The algorithm terminates if the iteration number exceeds I_1 or the solution stays unchanged.

The complexity of Alg. 1 falls in the sorting process in line 3 and the arg-max process in line 7. The complexity of sorting K users based on μ_{sk} and choosing the pattern with the largest value of ν_{sn} are $\mathcal{O}(K\log(K))$ and $\mathcal{O}(N)$, respectively [22]. Thus the overall complexity is derived as $\mathcal{O}(I_1 S(K\log(K)+N))$.

V. Joint Optimization of Power Allocation and User Scheduling

In this section, we jointly optimize power allocation and user scheduling given decided beam pattern selection and user association, which is expressed as,

$$\mathcal{P}_2 : \min_{P_{st}, x_{skt}} \sum_{k \in \mathcal{K}} |R_k - D_k| \quad (15a)$$

$$\text{s.t. } (11b), (11e), (11h). \quad (15b)$$

Note that only scheduled users with $\sum_{s \in \mathcal{S}} z_{sk} = 1$ are considered and hence contraints (11f) are omitted in $\mathcal{P}_2$. The problem is still in the format of mixed-integer nonconvex programming.

A. Problem Transformation

Solving $\mathcal{P}_2$ is complicated. Considering the applicability of the solution to practical implementation, we break the coupling across timeslots in $\mathcal{P}_2$ and decompose the problem into T subproblems, each of which corresponds to a timeslot. The subproblem at timeslot t is written as,

$$\mathcal{P}_2(t) : \min_{P_{st}, x_{skt}} \sum_{k \in \mathcal{K}} \left| \sum_{s \in \mathcal{S}} x_{skt} R_{skt} + \bar{R}_{kt} - D_k \right| + \rho \sum_{k \in \mathcal{K}} \left[R_k^{\min} - \sum_{s \in \mathcal{S}} x_{skt} R_{skt} - \bar{R}_{kt} \right]^+ \quad (16a)$$

$$\text{s.t. } P_{st} \leq \bar{P}_s, \forall s \in \mathcal{S}, \quad (16b)$$

$$\sum_{k \in \mathcal{K}} x_{skt} = 1, \forall s \in \mathcal{S}. \quad (16c)$$

Here, we define $\bar{R}_{kt}$ as the rate already allocated to the user before the t-th timeslot, which is expressed as,

$$\bar{R}_{kt} = \sum_{\tau=0}^{t-1} \sum_{s \in \mathcal{S}} x_{sk\tau} R_{sk\tau}, \quad (17)$$

where $R_{sk0} = 0$, $\forall s \in \mathcal{S}$, $\forall k \in \mathcal{K}$. We move constraints (11h) to the objective as a penalty with the factor $\rho > 0$. The operator $[\cdot]^+$ is equivalent to $\max\{\cdot, 0\}$. The objective is penalized if constraints (11h) are violated.

We convert $\mathcal{P}_2(t)$ into the following problem where the absolute operation in the objective is removed,

$$\mathcal{P}_2'(t) : \min_{P_{st}, x_{skt}} \sum_{k \in \mathcal{K}} \left(D_k - \sum_{s \in \mathcal{S}} x_{skt} R_{skt} - \bar{R}_{kt} \right) + \rho \sum_{k \in \mathcal{K}} \left[R_k^{\min} - \sum_{s \in \mathcal{S}} x_{skt} R_{skt} - \bar{R}_{kt} \right]^+ \quad (18a)$$

$$\text{s.t. } (16b), (16c),$$

$$\sum_{s \in \mathcal{S}} x_{skt} R_{skt} + \bar{R}_{kt} \leq D_k, \forall k \in \mathcal{K}. \quad (18b)$$

The equivalence between $\mathcal{P}_2(t)$ and $\mathcal{P}_2'(t)$ is built based on the following proposition, which conveys that if the resource is sufficient, the optimal allocated rates of the scheduled users are no larger than their demands.

Proposition 1: At the optimum of $\mathcal{P}_2(t)$, the allocated rates meet $\sum_{s \in \mathcal{S}} x_{skt} R_{skt} + \bar{R}_{kt} \leq D_k$, $\forall k \in \mathcal{K}$.

Proof. Please kindly refer to Appendix A. □

B. Algorithmic Design

To solve $\mathcal{P}_2'(t)$ with combinatorial and nonconvex properties, one of the widely-adopted ideas is to convert the problem into a series of convex subproblems, where the solution can be obtained by iteratively solving these subproblems. Conventional approaches, e.g., successive convex approximation

(SCA) method and Dinkelbach's transform method, can be applied. However, since a convex problem needs to be solved at each iteration, these approaches may end up with large computational complexity in practice. We design an iterative approach based on quadratic transform method [23] with lower complexity. One benefit of quadratic transform method is that the log-fractional rate functions can be converted into convex quadratic expressions and the series of convex subproblems can be optimized by deriving closed-formed update rules such that the overall complexity can be largely reduced.

We introduce auxiliary variables $\gamma_s \geq 0$ and $\eta_s \geq 0$ and transform the rate functions in (9) as the following,

$$\begin{aligned}\widetilde{R}_{skt} =& B\log(1+\gamma_s) - B\gamma_s + 2\eta_s\sqrt{B(1+\gamma_s)|h_{sk}|^2 P_{st}} \\ &- \eta_s^2 \sum_{s'\in\mathcal{S}} |h_{s'k}|^2 P_{s't} - \eta_s^2\sigma^2. \end{aligned} \tag{19}$$

By substituting $\widetilde{R}_{skt}$ into $\mathcal{P}_2'(t)$, the problem is then transformed into the following,

$$\begin{aligned}\mathcal{P}_2''(t): \min_{P_{st},x_{skt},\gamma_s,\eta_s} & \sum_{k\in\mathcal{K}} \left(D_k - \sum_{s\in\mathcal{S}} x_{skt}\widetilde{R}_{skt} - \bar{R}_{kt}\right) \\ &+ \rho \sum_{k\in\mathcal{K}} \left[R_k^{\min} - \sum_{s\in\mathcal{S}} x_{skt}\widetilde{R}_{skt} - \bar{R}_{kt}\right]^+ \quad (20a) \\ \text{s.t. } & (16b), (16c), (18b). \quad (20b)\end{aligned}$$

We derive an iterative approach to solve $\mathcal{P}_2''(t)$. Given x_{skt} and P_{st}, we update γ_s and η_s by,

$$\gamma_s = \frac{|h_{sk_s}|^2 P_{st}}{\sum_{s'\in\mathcal{S}\setminus\{s\}} |h_{s'k_s}|^2 P_{s't} + \sigma^2}, \tag{21}$$

$$\eta_s = \frac{B\sqrt{(1+\gamma_s)|h_{sk_s}|^2 P_{st}}}{\sum_{s'\in\mathcal{S}} |h_{s'k_s}|^2 P_{s't} + \sigma^2}, \tag{22}$$

where k_s denotes the index of the user scheduled by satellite s.

With fixed x_{skt}, γ_s, and η_s, the residual power allocation is convex without (18b), since the nonconvex rate functions have been converted to convex quadratic expressions. Thus, while the update iterates, we temporally ignore (18b). Power allocation will be adjusted to meet (18b) after the iterations. Note that only the S scheduled user with $x_{skt} = 1$ are considered at this phase and thus $\sum_{s\in\mathcal{S}} x_{skt}\widetilde{R}_{skt} = \widetilde{R}_{sk_st}$ in this case. The corresponding Lagrangian dual function is derived as,

$$\begin{aligned}\mathcal{L}(P_{st}) =& \sum_{s\in\mathcal{S}} (D_{k_s} - \widetilde{R}_{sk_st} - \bar{R}_{k_st}) \\ &+ \rho \sum_{s\in\mathcal{S}} \left[R_{k_s}^{\min} - \widetilde{R}_{sk_st} - \bar{R}_{k_st}\right]^+. \end{aligned} \tag{23}$$

The KKT conditions are,

$$\begin{aligned}\frac{\partial\mathcal{L}}{\partial P_{st}} =& (1+\psi_s)\eta_s\sqrt{\frac{B(1+\gamma_s)|h_{sk_s}|^2}{P_{st}}} \\ &- \sum_{s'\in\mathcal{S}} (1+\psi_{s'})\eta_{s'}^2 |h_{sk_{s'}}|^2 = 0, \forall s\in\mathcal{S}, \end{aligned} \tag{24}$$

(25)

where

$$\psi_s = \begin{cases}\rho, \text{ if } \widetilde{R}_{k_st} + \bar{R}_{k_st} < R_{k_s}^{\min}; \\ 0, \text{ if } \widetilde{R}_{k_st} + \bar{R}_{k_st} \geq R_{k_s}^{\min}.\end{cases} \tag{26}$$

Then the optimal power allocation is derived by,

$$P_{st}^* = \min\left\{\frac{(1+\psi_s)^2(\eta_s)^2 B(1+\gamma_s)|h_{sk_s}|^2}{\left(\sum_{s'\in\mathcal{S}}(1+\psi_{s'})\eta_{s'}^2|h_{sk_{s'}}|^2\right)^2}, \bar{P}_s\right\}. \tag{27}$$

The total number of potential combinations for deciding all ψ_s is 2^S. To maintain the computational complexity at an acceptable level, a heuristic decision strategy is applied. We first let $\psi_s = 1$ for all satellites and calculate P_{st} and $\widetilde{R}_{kt}$. Then set $\psi_s = \rho$ to increase the power value (let $P_{st} = \bar{P}_{st}$ when P_s surpasses the budget) if $\widetilde{R}_{k_st} + \bar{R}_{k_st} < R_{k_s}^{\min}$.

As the power allocation is decided, we can calculate $\widetilde{R}_{skt}$ for each user. The residual user scheduling problem is a linear integer programming, which can be further divided into each satellite as,

$$\begin{aligned}\mathcal{P}_3''(t,s): \min_{x_{skt}} & \sum_{k\in\mathcal{K}_s} \left(D_k - x_{skt}\widetilde{R}_{skt} - \bar{R}_{kt}\right) \\ &+ \rho \sum_{k\in\mathcal{K}_s} \left[R_k^{\min} - x_{skt}\widetilde{R}_{skt} - \bar{R}_{kt}\right]^+ \quad (28a) \\ \text{s.t. } & \sum_{k\in\mathcal{K}} x_{skt} = 1, \quad (28b)\end{aligned}$$

where $\mathcal{K}_s$ is the set containing the users associated to satellite s but excluding users already satisfied with demands. With (28b) that each satellite can only schedule one user to each timeslot, we can derive the following rule to select the optimal user for the s-th satellite,

$$k_s^* = \arg\min_{k\in\mathcal{K}_s} D_k - \widetilde{R}_{skt} - \bar{R}_{kt} + \rho\left[R_k^{\min} - \widetilde{R}_{skt} - \bar{R}_{kt}\right]^+. \tag{29}$$

Then we set $x_{sk_s^*t} = 1$ accordingly.

After iterations, we need to adjust the power allocation to meet constraints (18b). Let $\bar{\mathcal{S}}$ be the set of the satellites whose scheduled users' rates are larger than their demands, i.e., $R_{k_st} + \bar{R}_{k_st} > D_{k_s}$. We set $R_{k_st} = D_{k_s} - \bar{R}_{k_st}$, $\forall s\in\bar{\mathcal{S}}$, and convert the corresponding rate expressions into the following,

$$P_{st} = \left(2^{\frac{R_{k_st}}{B}} - 1\right)\frac{\sum_{s'\in\mathcal{S}\setminus\{s\}} |h_{s'k_s}|^2 P_{s't} + \sigma^2}{|h_{sk_s}|^2}, \forall s\in\mathcal{S}, \tag{30}$$

which can be viewed as the equations of P_{st}. By solving the equations, the power allocation for those users can be adjusted to $R_{k_st} + \bar{R}_{k_st} = D_{k_s}$. After that, we need to remove users with satisfied demands from $\mathcal{K}_s$.

The whole procedure of jointly optimizing power allocation and user scheduling is summarized in Alg. 2. The algorithm is operated timeslot by timeslot. In each timeslot, iterations are performed to update γ_s, η_s, P_{st}, and x_{skt} from line 4 to line 7, and terminate when convergence occurs or the maximum number of iterations I_2 is reached. Within each iteration, the update of x_{skt} (computing the values in (29) and selecting the user with the minimum for each satellite) dominates the complexity with $\mathcal{O}(S\widetilde{K})$. In line 10, power

Algorithm 2 Joint optimization of power allocation and user scheduling

Input: y_{sn}, z_{sk}, ρ, D_k, $\mathcal{K}_s$, and channel gains; Initialized P_{st} and x_{skt}.

1: **for** $t = 1, \ldots, T$ **do**
2: Initialize γ_s and η_s, $\forall s \in \mathcal{S}$.
3: **repeat**
4: Update γ_s and η_s in (21) and (22), respectively.
5: Compute P_{st} in (27) by letting $\psi_s = 1$, $\forall s \in \mathcal{S}$.
6: Adjust P_{st} in (27) with $\psi_s = \rho$ for satellites with $\widetilde{R}_{kt} + \bar{R}_{kt} < R_k^{\min}$.
7: Update x_{skt} based on the rule in (29).
8: **until** Convergence or reaching I_2 iterations
9: **if** there exist users with $R_{kt} + \bar{R}_{kt} > D_k$ **then**
10: Set $R_{k_s t} + \bar{R}_{k_s t} = D_{k_s}$ for these users and adjust P_{st} by solving equations in (30).
11: **end if**
12: Update $\mathcal{K}_s$ and calculate $\bar{R}_{kt}$.
13: **end for**

Output: Optimized P_{st} and x_{skt}.

allocation is adjusted to meet $R_k \leq D_k$, where the complexity of solving the equations in (30) is $\mathcal{O}(S^3)$ [24] in the worst case. Thus, the complexity of Alg. 2 is $\mathcal{O}(T(I_2 S\widetilde{K} + S^3))$.

C. The Algorithm Framework

To solve $\mathcal{P}_0$, Alg. 1 is performed first to decide beam patterns and user association at the frame level and then Alg. 2 is executed to jointly optimize power allocation and user scheduling at the timeslot level. To futher improve the performance, we design a swap-based algorithm to update the selection of beam patterns and users to iteratively decrease the capacity-demand gap.

Beam pattern selection and user association can be defined as two many-to-one matching problems. A swap of satellite-pattern matching is defined as $\Phi_{sn'}^{sn}$, denoting that satellite s changes pattern selection from n to n'. In other words, the integer solution changes from $\{y_{sn} = 1, y_{sn'} = 0\}$ to $\{y_{sn} = 0, y_{sn'} = 1\}$. Similarly, we define a swap of satellite-user matching as $\Psi_{sk'}^{sk}$, which means the satellite changes the scheduling from user k to user k'. Accordingly, the integer solution of $\{z_{sk} = 1, z_{sk'} = 0\}$ is changed to $\{z_{sk} = 0, z_{sk'} = 1\}$. The swaps $\Phi_{sn'}^{sn}$ and $\Psi_{sk'}^{sk}$ are operated if:

- $\mathcal{F} > \mathcal{F}'$, where $\mathcal{F}$ and $\mathcal{F}'$ are the objective values before and after the swaps, respectively.

The detailed procedure of the overall scheme is summarized in Alg. 3. In line 1, beam pattern selection and user association are initialized by Alg. 1. From line 2 to line 9, the update operation is executed for I_3 iterations. Within each iteration, we first randomly select swaps in line 3 and calculate the objective value based on the satellite-pattern and satellite-user matchings after the swaps by optimizing power allocation and user scheduling via Alg. 2 in line 4. In line 5 to line 8, we operate the swaps and update the best solution and objective value if the capacity-demand gap decreases after the swaps. The complexity of each iteration mainly comes from executing Alg. 1. Thus the overall complexity of Alg. 3 is $\mathcal{O}(I_3 T(I_2 S\widetilde{K} + S^3))$.

Algorithm 3 Joint optimization of adaptive beam patterns and resource allocation

Input: D_k and channel gains; Initialized $\mathcal{F}^* = \inf$ as the best objective value, x_{skt}^*, y_{sn}^*, z_{sk}^*, and P_{st}^* as the best solution.

1: Determine beam pattern selection and user association by Alg. 1 and update y_{sn}^* and z_{sk}^*.
2: **repeat**
3: Randomly select swaps $\Phi_{sn'}^{sn}$ and $\Psi_{sk'}^{sk}$, where y_{sn} and z_{sk} are the solution after this swap.
4: Optimize power allocation and user scheduling by Alg. 2 based on y_{sn} and z_{sk}. Obtain x_{skt}, P_{st}, and the corresponding objective value $\mathcal{F}$.
5: **if** $\mathcal{F} < \mathcal{F}^*$ **then**
6: Operate the swaps.
7: Update $x_{skt}^* = x_{skt}$, $y_{sn}^* = y_{sn}$, $z_{sk}^* = z_{sk}$, $P_{st}^* = P_{st}$, and $\mathcal{F}^* = \mathcal{F}$.
8: **end if**
9: **until** Reaching I_3 iterations

Output: x_{skt}^*, y_{sn}^*, z_{sk}^*, and P_{st}^*.

TABLE I: Simulation parameters

Parameter	Value
Frequency, f^{freq}	20 GHz
Bandwidth, W	400 MHz
Satellite height	600 km
Number of satellites, S	5
Power budget, P_s	43 dBm
Number of beam patterns, N	5
Receive antenna gain, G_k^{Rx}	35 dBi
Noise power, σ^2	-126.47 dBW
Number of timeslots, T	32
Minimum elevation angle	40°
Minimum association rate, $R_k^{\min}$	100 kbps
Number of iterations, I_1, I_2, I_3	10, 30, 50

For practical implementation, the algorithm can be divided into two parts. With less flexibility compared to power allocation and user scheduling, the optimization of user association and beam pattern selection can be solved ahead of service with predicted channel models and demands for a long-term goal of diminishing capacity-demand gap. During each frame, dynamic issues may happen. In this case, user scheduling and power allocation can be optimized in a short-term way to adapt to short-term changes.

VI. Numerical Results

In simulation, we consider a square area with 200×200 km^2, where the generation of users follows two-dimension normal distributions [25]. The main parameters are summarized in Table I, unless otherwise stated. The generation of beam radiation patterns follows the rule in [7] and [10] where $G_{sn,\max}^{\text{Tx}}$ depends on the beamwidth. We consider beam patterns which generate circular beams with 3-dB beamwidths $\{1°, 1.5°, 2°, 2.5°, 3°\}$ [7]. Beams with 1° beamwidth have the largest directivity to the beam center whereas those with 3°

beamwidth generate the widest service range. The results are averaged over 500 instances.

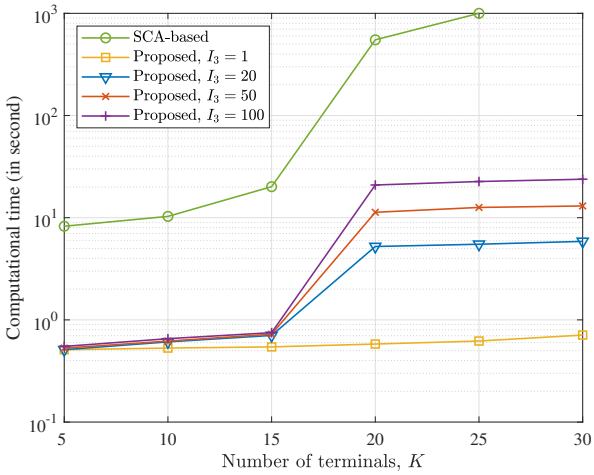

Fig. 5: Average computational time consumed by the proposed approaches (with different I_3) and the SCA-based approach.

We first evaluate the performance of the proposed approach in the aspects of consumed computational time in Fig. 5. For comparison, a benchmark based on the conventional convexification (SCA) method is set, where the power optimization problem is addressed by solving a series of approximated convex subproblems and the integer solution is obtained by Alg. 3 with $I_3 = 50$. We can observe that the proposed approach can maintain the computational time at the level of milliseconds when $K \leq 15$. This is because resources are enough to satisfy users' demand when the number of users is small such that the algorithm can perform an early stop. As the problem size increases with the number of users ($K \geq 20$), the consumed computational time of the proposed approach remains a relatively smooth variation compared to the SCA-based approach. When $I_3 = 1$, the computational time stays below 1 second since no update of integer solutions is executed. The SCA-based approach requires more computational time with a drastic rise. As described in Alg. 2, we jointly optimize power allocation and user scheduling by a series of closed-form expressions rather than solving convex subproblems, which saves up computational efforts compared to the conventional SCA-based scheme.

In Fig. 6, we present the capacity-demand gap performance of the proposed and SCA-based schemes. As abovementioned, users' capacity matches to their requested demand when $K \leq 15$. After that, the capacity-demand gap grows with K linearly. With swap-based update of beam pattern selection and user association, the proposed scheme with $I_3 = 20$ can alleviate the mismatch by 39.81% over that with $I_3 = 1$. As the number of iterations I_3 increases, the proposed scheme reduces the capacity-demand gap through searching more possible integer solutions but tends to converge. From $I_3 = 20$ to 50, the proposed approach decreases the gap by 12.40%. The reduction is 6.95% when I_3 rises from 50 to 100. Compared to the SCA-based approach, the proposed approach only sacrifices 4.11% performance but largely reduces the computational

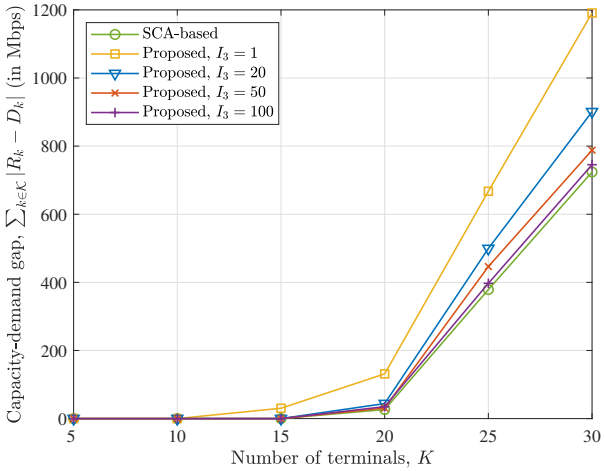

Fig. 6: Gap performance of the proposed schemes (with different I_3) and the SCA-based approach versus the number of users K (average demand is set to be 200 Mbps).

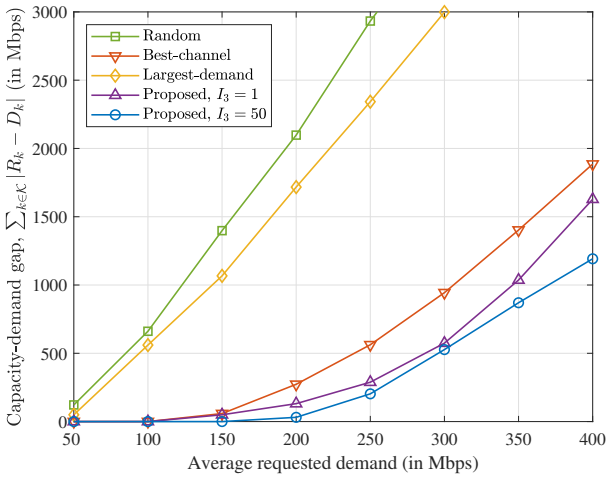

Fig. 7: Gap performance of the proposed scheme and state-of-the-art strategies, where $K = 20$.

efforts as presented in Fig. 5, which demonstrates a better complexity-performance tradeoff.

Then we compare the proposed scheme with some state-of-the-art strategies in Fig. 7. We set the following strategies as benchmarks:

- Random: Each satellite selects $\widetilde{K}$ users for association randomly and then chooses the beam pattern with the largest ν_{sn}. At each timeslot, users are scheduled following the Round-Robin basis [26].
- Best-channel: users are associated to satellites with the best channel gains and beam patterns with the largest ν_{sn} are selected. During the scheduling period, each satellite serves best-channel users first until $R_k \geq D_k$ [4], [27].
- Largest-demand: Each satellite chooses users with the largest demand and then select the largest-ν_{sn} patterns. Timeslots are scheduled to users with largest demand first.

Note that power allocation is optimized following Alg. 2 in

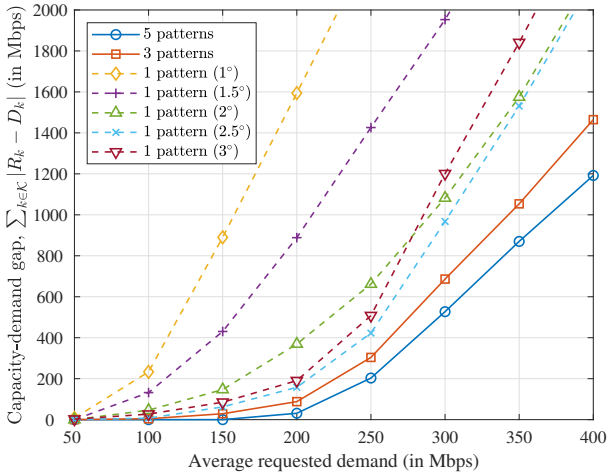

Fig. 8: Gap performance of the schemes with different beam pattern settings, where $K = 20$.

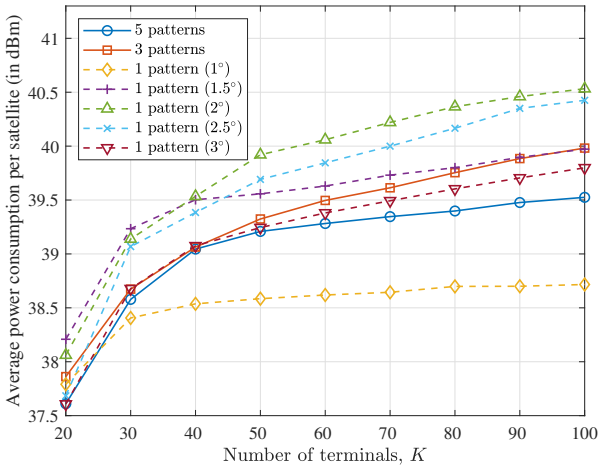

Fig. 9: Power consumption of the schemes with different beam pattern settings, where the average demand is 200 Mbps.

the above benchmarks. Among benchmarks, the Best-channel scheme outperforms the other two but yields larger capacity-demand mismatch over the proposed schemes. This is because the proposed schemes consider both users' channel conditions and demand when deciding user association and perform joint optimization of power allocation and user scheduling. Compared to the Best-channel scheme, the proposed schemes reduce the capacity-demand gap by 27.67% and 44.92% when $I_3 = 1$ and $I_3 = 50$, respectively.

Next, we evaluate the capacity-demand gap performance of the approaches with different beam pattern settings (5 patterns, 3 patterns, and 1 pattern) in Fig. 8. In the 3-pattern scheme, each satellite can generate beams with 3-dB beamwidths $\{1°, 2°, 3°\}$. As for schemes with single pattern, Alg. 1 is employed to decide user association and then Alg. 2 is adopted to perform power and user scheduling. The resulted capacity-demand gap increases with the growth of the average requested demand. Among single-pattern schemes, the one with $2.5°$ beamwidth outperforms the others. Functioned with multiple beam patterns, 3-pattern and 5-pattern schemes improve the capability of meeting users' demand, with 31.46% and 46.68% reduction of capacity-demand gap over the single-pattern scheme with $2.5°$ beamwidth, respectively.

In Fig. 9, we evaluate the average power consumption per satellite of different schemes. Generally, the power consumption rises with the number of users K but tends to be steady when K is large. Particularly, the single-pattern scheme with $1°$ beamwidth results in the least power consumption in spite of the worst performance in reducing capacity-demand gap. With more flexibility introduced in spatial domain, the 5-pattern scheme can guarantee good capacity-demand matching with power consumption smaller than the other four single-pattern schemes. Moreover, the capability of user association of different schemes is presented in Fig. 10. Compared to the single-pattern scheme with $2°$ beamwidth, which performs the best with the most associated users, the 5-pattern and 3-pattern schemes sacrify 8.04% and 10.13% performance, respectively. The designed multiple-pattern scheme can achieve

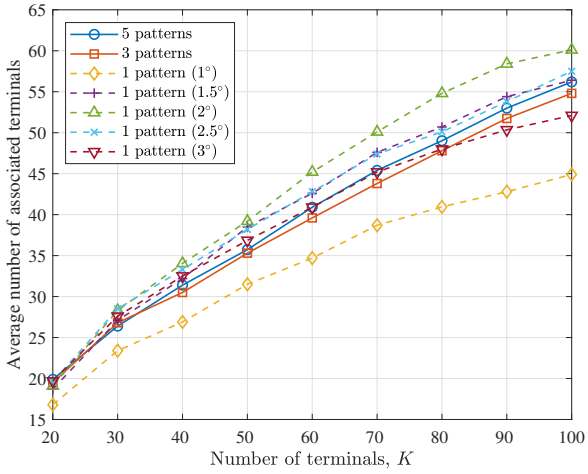

Fig. 10: Average number of associated users (with $R_k \geq R_k^{\min}$) achieved by the schemes with different beam pattern settings, where the average demand is 200 Mbps.

a good balance between capacity-demand matching and power consumption/user association over conventional single-pattern schemes.

In practical systems, LEO satellites equipped with advanced payloads (adopting the multiple-pattern scheme) would coexist with those equipped with conventional payloads (using the single-pattern scheme). We evaluate the performance of scenarios with different types of satellite payloads in Fig. 11. The more satellites are equipped with multiple beam patterns, the more spatial-domain flexibility is offered and thus the more reduction in capacity-demand gap is obtained. By introducing adaptive beam patterns, the capacity-demand gap is largely reduced by 91.59% and 76.19% when $N = 5$ and $N = 3$, respectively.

VII. Conclusion

In this paper, we have investigated joint resource optimization and discussed synergies of spatial-temporal domain flex-

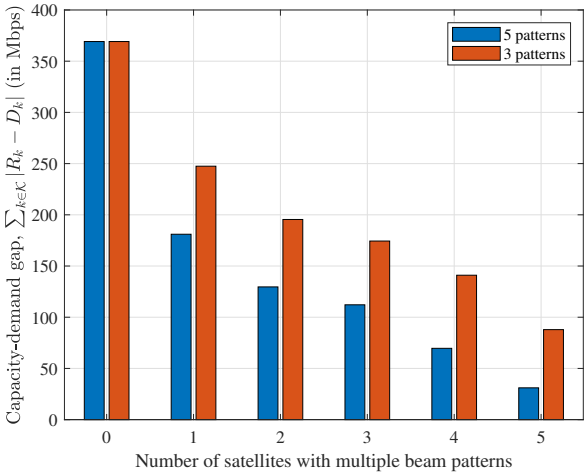

Fig. 11: Gap performance of LEO satellite systems with the coexistence of satellite payloads with both conventional single pattern and multiple patterns. Note that beamwidth is set to 2° in the single-pattern scheme. Here, the average demand is 200 Mbps and $K = 20$.

ibilities when adopting adaptive beam patterns with flexible user scheduling in LEO satellite systems. We have designed an algorithmic framework to first determine beam pattern selection and user-LEO association, and then jointly optimize user-slot scheduling and power allocation. We have revealed facts for guiding algorithm design. That is, to mitigate the mismatch effect, users with better channel and high demand are prone to be served by narrow beams with low radiated interference to other users. Furthermore, we have proposed a swap-based update strategy to iteratively reduce the capacity-demand gap. Numerical results have demonstrated a good tradeoff of the designed scheme between performance and complexity and the advanced capability of matching capacity to demand when extra flexibility in spatial domain is introduced.

APPENDIX

A. Proof of Proposition 1

We prove the proposition by contradiction. Assume that there exist users with $\sum_{s\in\mathcal{S}} x_{skt}R_{skt} + \bar{R}_{kt} > D_k$ at the optimum of $\mathcal{P}_2(t)$. Denote S_t^+ and S_t^- as the sets of satellites offering their scheduled users with $\sum_{s\in\mathcal{S}} x_{skt}R_{skt} + \bar{R}_{kt} > D_k$ and $\sum_{s\in\mathcal{S}} x_{skt}R_{skt} + \bar{R}_{kt} \le D_k$, respectively. Let P_{st}^* be the optimal power allocation and ϱ control the power of users scheduled by satellites in S_t^+. Note that, at the optimum, ϱ is set to 1. For users scheduled by satellites in S_t^+, the optimal SINR expression is derived as,

$$\gamma_{skt} = \frac{|h_{sk}|^2 \varrho P_{st}^*}{\sum\limits_{s'\in\mathcal{S}_t^+\setminus\{s\}} |h_{s'k}|^2 \varrho P_{s't}^* + \sum\limits_{s'\in\mathcal{S}_t^-} |h_{s'k}|^2 P_{s't}^* + \sigma^2}, \tag{31}$$

Similarly, the optimal SINR of users scheduled by satellites in S_t^- is expressed as,

$$\gamma_{skt} = \frac{|h_{sk}|^2 P_{st}^*}{\sum\limits_{s'\in\mathcal{S}_t^+} |h_{s'k}|^2 \varrho P_{s't}^* + \sum\limits_{s'\in\mathcal{S}_t^-\setminus\{s\}} |h_{s'k}|^2 P_{s't}^* + \sigma^2}, \tag{32}$$

With the optimal P_{st}^*, we view the objective as the function of ϱ and derive the derivative of the objective regarding ϱ in (33). Note that

$$\bar{\rho} = \begin{cases} \rho, & \text{if } R_k^{\min} > \sum_{s\in\mathcal{S}} x_{skt}R_{skt} + \bar{R}_{kt}; \\ 0, & \text{otherwise.} \end{cases} \tag{34}$$

We can observe that the derivative of the objective with respect to ϱ is larger than 0. This result conveys that the objective value could be smaller if we lower transmit power of satellites in $\mathcal{S}_t^+$ by reducing ϱ, which is contrary the assumption of optimality. Hence the proposition.

REFERENCES

[1] F. Rinaldi, H.-L. Maattanen, J. Torsner, S. Pizzi, S. Andreev, A. Iera, Y. Koucheryavy, and G. Araniti, "Non-terrestrial networks in 5G & beyond: A survey," *IEEE Access*, vol. 8, pp. 165 178–165 200, 2020.

[2] O. Kodheli, E. Lagunas, N. Maturo, S. K. Sharma, B. Shankar, J. F. M. Montoya, J. C. M. Duncan, D. Spano, S. Chatzinotas, S. Kisseleff *et al.*, "Satellite communications in the new space era: A survey and future challenges," *IEEE Communications Surveys & Tutorials*, vol. 23, no. 1, pp. 70–109, 2020.

[3] V. L. Foreman, A. Siddiqi, and O. De Weck, "Large satellite constellation orbital debris impacts: Case studies of oneweb and spacex proposals," in *AIAA SPACE and Astronautics Forum and Exposition*, 2017, pp. 5200.

[4] M. Y. Abdelsadek, H. Yanikomeroglu, and G. K. Kurt, "Future ultra-dense LEO satellite networks: A cell-free massive MIMO approach," in *2021 IEEE International Conference on Communications Workshops (ICC Workshops)*. IEEE, 2021, pp. 1–6.

[5] B. Di, H. Zhang, L. Song, Y. Li, and G. Y. Li, "Ultra-dense LEO: Integrating terrestrial-satellite networks into 5G and beyond for data offloading," *IEEE Transactions on Wireless Communications*, vol. 18, no. 1, pp. 47–62, 2018.

[6] H. Al-Hraishawi, H. Chougrani, S. Kisseleff, E. Lagunas and S. Chatzinotas, "A Survey on Nongeostationary Satellite Systems: The Communication Perspective," in *IEEE Communications Surveys & Tutorials*, vol. 25, no. 1, pp. 101-132, Firstquarter 2023

[7] G. Maral, M. Bousquet, and Z. Sun, *Satellite communications systems: Systems, techniques and technology*. John Wiley & Sons, 2020.

[8] K. Y. Zhong, Y. J. Cheng, H. N. Yang, and B. Zheng, "LEO satellite multibeam coverage area division and beamforming method," *IEEE Antennas and Wireless Propagation Letters*, vol. 20, no. 11, pp. 2115–2119, 2021.

[9] Y. Su, Y. Liu, Y. Zhou, J. Yuan, H. Cao, and J. Shi, "Broadband LEO satellite communications: Architectures and key technologies," *IEEE Wireless Communications*, vol. 26, no. 2, pp. 55–61, 2019.

[10] M. Takahashi, Y. Kawamoto, N. Kato, A. Miura, and M. Toyoshima, "Adaptive power resource allocation with multi-beam directivity control in high-throughput satellite communication systems," *IEEE Wireless Communications Letters*, vol. 8, no. 4, pp. 1248–1251, 2019.

[11] G. Angus, R. Li, and V. MakHau, "FlexBeamOpt: Hybrid solution methodologies for highthroughput GEO satellite beam laydown and resource allocation," *International Journal of Satellite Communications and Networking*, 2023.

[12] P. J. Honnaiah, N. Maturo, S. Chatzinotas, S. Kisseleff, and J. Krause, "Demand-based adaptive multi-beam pattern and footprint planning for high throughput GEO satellite systems," *IEEE Open Journal of the Communications Society*, vol. 2, pp. 1526–1540, 2021.

[13] V-P. J. Andrs, J. Querol, F. Ortz, J. L. G. Rios, E. Lagunas, V. M. Baeza, G. Fontanesi, L. M. Garcs-Socorrs, J. C. M. Duncan, and S. Chatzinotas, "Flexible beamforming for direct radiating arrays in satellite communications," *IEEE Access*, 2023.

[14] F. G. Ortiz-Gomez, M. A. Salas-Natera, R. Martínez, and S. Landeros-Ayala, "Optimization in VHTS satellite system design with irregular beam coverage for non-uniform traffic distribution," *Remote Sensing*, vol. 13, no. 13, p. 2642, 2021.

[15] H. Chaker, H. Chougrani, W. A. Martins, S. Chatzinotas, and J. Grotz. "Matching traffic demand in geo multibeam satellites: The joint use of dynamic beamforming and precoding under practical constraints," *IEEE Transactions on Broadcasting*, vol. 68, no. 4 , p. 819–833, 2022.

$$\sum_{s\in\mathcal{S}_t^-}\sum_{k\in\mathcal{K}}\frac{x_{skt}\frac{(1+\bar{\rho}_{skt})\gamma_{skt}}{\varrho(1+\gamma_{skt})}\sum\limits_{s'\in\mathcal{S}_t^+}|h_{s'k}|^2P^*_{s't}}{\sum\limits_{s'\in\mathcal{S}_t^+}|h_{s'k}|^2\varrho P^*_{s't}+\sum\limits_{s'\in\mathcal{S}_t^-\setminus\{s\}}|h_{s'k}|^2P^*_{s't}+\sigma^2}+\sum_{s\in\mathcal{S}_t^+}\sum_{k\in\mathcal{K}}\frac{x_{skt}\frac{\gamma_{skt}}{\varrho(1+\gamma_{skt})}\left(\sum\limits_{s'\in\mathcal{S}_t^-\setminus\{s\}}|h_{s'k}|^2P^*_{s't}+\sigma^2\right)}{\sum\limits_{s'\in\mathcal{S}_t^+}|h_{s'k}|^2\varrho P^*_{s't}+\sum\limits_{s'\in\mathcal{S}_t^-\setminus\{s\}}|h_{s'k}|^2P^*_{s't}+\sigma^2} \quad (33)$$

[16] S. Tani, K. Motoyoshi, H. Sano, A. Okamura, H. Nishiyama, and N. Kato, "An adaptive beam control technique for Q band satellite to maximize diversity gain and mitigate interference to terrestrial networks," *IEEE Transactions on Emerging Topics in Computing*, vol. 7, no. 1, pp. 115–122, 2016.

[17] A. Guidotti, "Beam size design for new radio satellite communications systems," *IEEE Transactions on Vehicular Technology*, vol. 68, no. 11, pp. 11 379–11 383, 2019.

[18] X. Hu, Y. Zhang, X. Liao, Z. Liu, W. Wang and F. M. Ghannouchi, "Dynamic Beam Hopping Method Based on Multi-Objective Deep Reinforcement Learning for Next Generation Satellite Broadband Systems," *IEEE Transactions on Broadcasting*, vol. 66, no. 3, pp. 630-646, Sept. 2020.

[19] F. G. Ortíz-Gómez, R. M. Rodríguez-Osorio, M. Salas-Natera, and S. Landeros-Ayala, "Adaptive resources allocation for flexible payload enabling VHTS systems: Methodology and architecture," in *36th International Communications Satellite Systems Conference (ICSSC 2018)*. IET, 2018, pp. 1–8.

[20] A. Wang, L. Lei, X. Hu, E. Lagunas, A. I. Perez-Neira, and S. Chatzinotas, "Adaptive beam pattern selection and resource allocation for NOMA-based LEO satellite systems," in Proc. *IEEE Global Communications Conference (GLOBECOM)*, Dec. 2022, pp. 1–6, 2022.

[21] 3GPP TR 38.811, "Technical specification group radio access network: Study on new radio (NR) to support non-terrestrial networks (Release 15), v15.4.0," 2020.

[22] T. H. Cormen, C. E. Leiserson, R. L. Rivest, and C. Stein, *Introduction to algorithms*. MIT press, 2022.

[23] K. Shen and W. Yu, "Fractional programming for communication systems Part I: Power control and beamforming," *IEEE Transactions on Signal Processing*, vol. 66, no. 10, pp. 2616–2630, 2018.

[24] G. H. Golub and C. F. Van Loan, *Matrix computations*. JHU press, 2013.

[25] S. Xia, Q. Jiang, C. Zou, and G. Li, "Beam coverage comparison of LEO satellite systems based on user diversification," *IEEE access*, vol. 7, pp. 181 656–181 667, 2019.

[26] L. You, K.-X. Li, J. Wang, X. Gao, X.-G. Xia, and B. Ottersten, "Massive MIMO transmission for LEO satellite communications," *IEEE Journal on Selected Areas in Communications*, vol. 38, no. 8, pp. 1851–1865, 2020.

[27] T. Zhou, Z. Liu, J. Zhao, C. Li, and L. Yang, "Joint user association and power control for load balancing in downlink heterogeneous cellular networks," *IEEE Transactions on Vehicular Technology*, vol. 67, no. 3, pp. 2582–2593, 2017.